OMTN, Volume *29*

Supplemental information

Effective gene therapy of Stargardt disease with PEG-ECO/*pGRK1-ABCA4-S/MAR* nanoparticles

Da Sun, Wenyu Sun, Song-Qi Gao, Jonathan Lehrer, Amirreza Naderi, Cheng Wei, Sangjoon Lee, Andrew L. Schilb, Josef Scheidt, Ryan C. Hall, Elias I. Traboulsi, Krzysztof Palczewski, and Zheng-Rong Lu

SUPPLEMENTARY INFORMATION

Effective Gene Therapy of Stargardt Disease with PEG-ECO/*pGRK1-ABCA4-S/MAR* Nanoparticles

1. Construction of *ABCA4* plasmid DNA with the human *GRK1* promoter, human beta-Globin *polyA* and human *S/MAR* enhancer.

Previously, we have demonstrated excellent efficacy using our ECO-based gene therapy platform involving a therapeutic plasmid with a bovine rhodopsin promoter and an enhancer with viral origin [1, 2]. Here, a new *ABCA4* plasmid DNA with a human promoter and enhancer has been constructed to promote specific expression of ABCA4 in both cone and rod photoreceptors for possible clinical use. A DNA fragment of the human *GRK1* (-109 to + 183) promoter and a beta-Globin *polyA* were amplified from human genomic DNA, according to a previous work [3]. A human scaffold/matrix attachment region enhancer (*S/MAR*) DNA was also incorporated in the plasmid construct to enhance/prolong gene expression. The *GRK1* promoter was inserted into *MluI* and *AgeI* restriction sites, while the *polyA* and *S/MAR* DNA were inserted into *NotI* and *NheI* restriction sites. The whole plasmid maps of *pGRK1-ABCA4-S/MAR* and control plasmids *pRHO-ABCA4* and *pGRK1-ABCA4 without S/MAR* are shown in **Fig. S1A**. The respective plasmid structures were confirmed by digestion with multiple restriction enzymes and agarose gel electrophoresis (**Fig. S1B)**. Four restriction enzymes, *MluI, AgeI*, *NotI* and *NheI*, were used in multiple enzyme digestion reactions. Agarose gel (1%) was prepared to separate 4 DNA fragments after digestion. In this new therapeutic plasmid, promoter *GRK1* (300 bp), *ABCA4* (6.8 kb), *polyA*+*S/MAR* (2.9 kb) and vector backbone (~2.5 kb) were separated after digestion and gel electrophoresis. While building the therapeutic construct, we further deleted some non-essential sequences from vector and reduced size of vector backbone to 2.5 kb. The electrophoresis results confirmed the success of plasmid construction. Full length sequencing was also performed on the new *ABCA4* plasmid.

After modification, a similar *ABCA4* expression level in *Abca4*$^{-/-}$ mice was observed with the *GRK1* promoter as with the *RHO* promoter (**Fig. S1C)**. The addition of the *S/MAR* enhancer facilitated similar *ABCA4* mRNA expression 1 week after treatment, compared to without

S/MAR. However, significantly prolonged expression was observed 1 month after treatment, compared to no enhancer control, demonstrating gene expression enhancement effect for a longer time (**Fig. S1D)**.

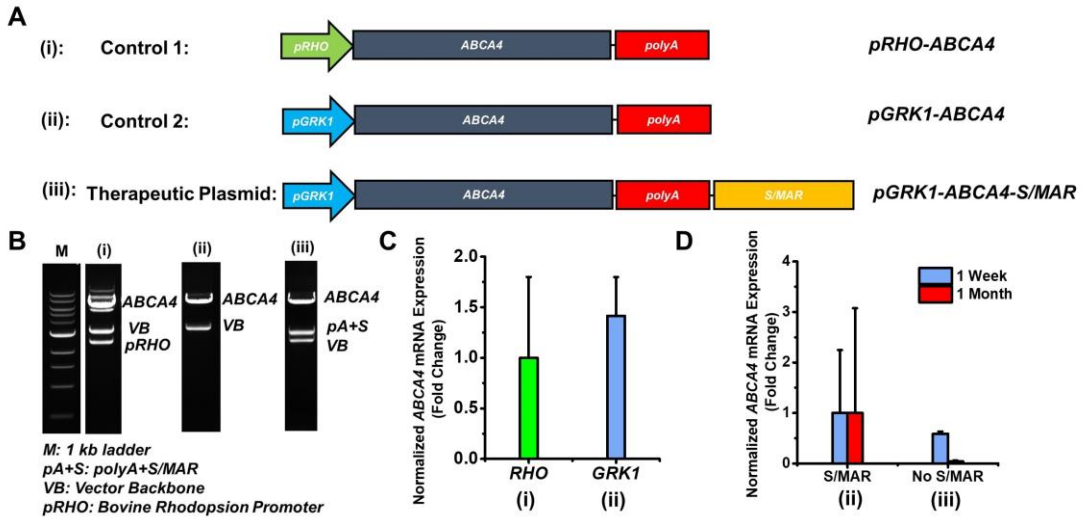

Fig. S1. Therapeutic plasmid construction, structure confirmation, and characterization of expression. (A) Diagram of functional components, **(B)** agarose gel electrophoresis of multiple restriction-enzyme digestion to verify correct-sized DNA fragments of (i) control pRHO-ABCA4; (ii) pGRK1-ABCA4; and (iii) therapeutic *pGRK1-ABCA4-SMAR*. The *GRK1* promoter was inserted between *MluI* and *AgeI* restriction sites. *ABCA4* mRNA expression in *Abca4*$^{-/-}$ mice 1 week or 1 month after subretinal administration of ECO/pDNA nanoparticles (100 ng/eye), using plasmids with different promoters **(C)** (i) and (ii); or **(D)** with (ii) and without(iii) *S/MAR* enhancer modification.

2. Characterization of ECO/*pGRK1-ABCA4-S/MAR* nanoparticles

All the ECO/*pDNA* nanoparticle formulations were formulated as described in the materials and methods section. Sucrose (10%) was added to the nanoparticle solution after formulation. The sizes and zeta potentials were evaluated also as described in the materials and methods section. Agarose gel electrophoresis was used to evaluate the encapsulation and stability of the formulations of ECO/*pGRK1-ABCA4-S/MAR* nanoparticles, either fresh made or under different storage conditions (4℃ and -20 ℃). Encapsulated DNA will reduce mobility

when nanoparticles are formed. Specifically, 4 formulations were tested: **(i)** ECO/*pGRK1-ABCA4-S/MAR,* **(ii)** ECO/*pGRK1-ABCA4-S/MAR* (10% sucrose) **(iii)** PEG-ECO/*pGRK1-ABCA4-S/MAR,* and **(iv)** PEG-ECO/*pGRK1-ABCA4-S/MAR* (10% sucrose). Results are displayed in **Fig. S2.** All the nanoparticles demonstrated efficient *pDNA* encapsulation and excellent stability for 1 week and 1 month after storage at 4℃ or -20 ℃, indicated by the bright bands on the top of each agarose electrophoresis gel (**Fig. S2)**.

Dynamic light scattering (DLS) of size distributions from the formulations of ECO/*pGRK1-ABCA4-S/MAR* nanoparticles were summarized in **Fig. S2D**. **(i)** ECO/*pGRK1-ABCA4-S/MAR* nanoparticles demonstrated good stability until aggregations formation after a month storage under -20 ℃, where a wider size distribution was shown. There was no significant change in the size distribution observed for **(ii)** ECO/*pGRK1-ABCA4-S/MAR* (10% sucrose)*,* **(iii)** PEG-ECO/*pGRK1-ABCA4-S/MAR* and **(iv)** PEG-ECO/*pGRK1-ABCA4-S/MAR* (10% sucrose) nanoparticles **Fig. S2D**. The sizes and zeta potentials are summarized also in **Table S1.** All the nanoparticle formulations demonstrated consistent sizes (150 nm~200 nm) and proper positive zeta potentials (+15 mV~45 mV). The effect of storage on expression was also evaluated. No change was observed after 45 days of storage of the same nanoparticle formulation, and significant transfection efficiency was retained for the formulation after storage at -20℃ for 70 days (**Fig. S2E)**.

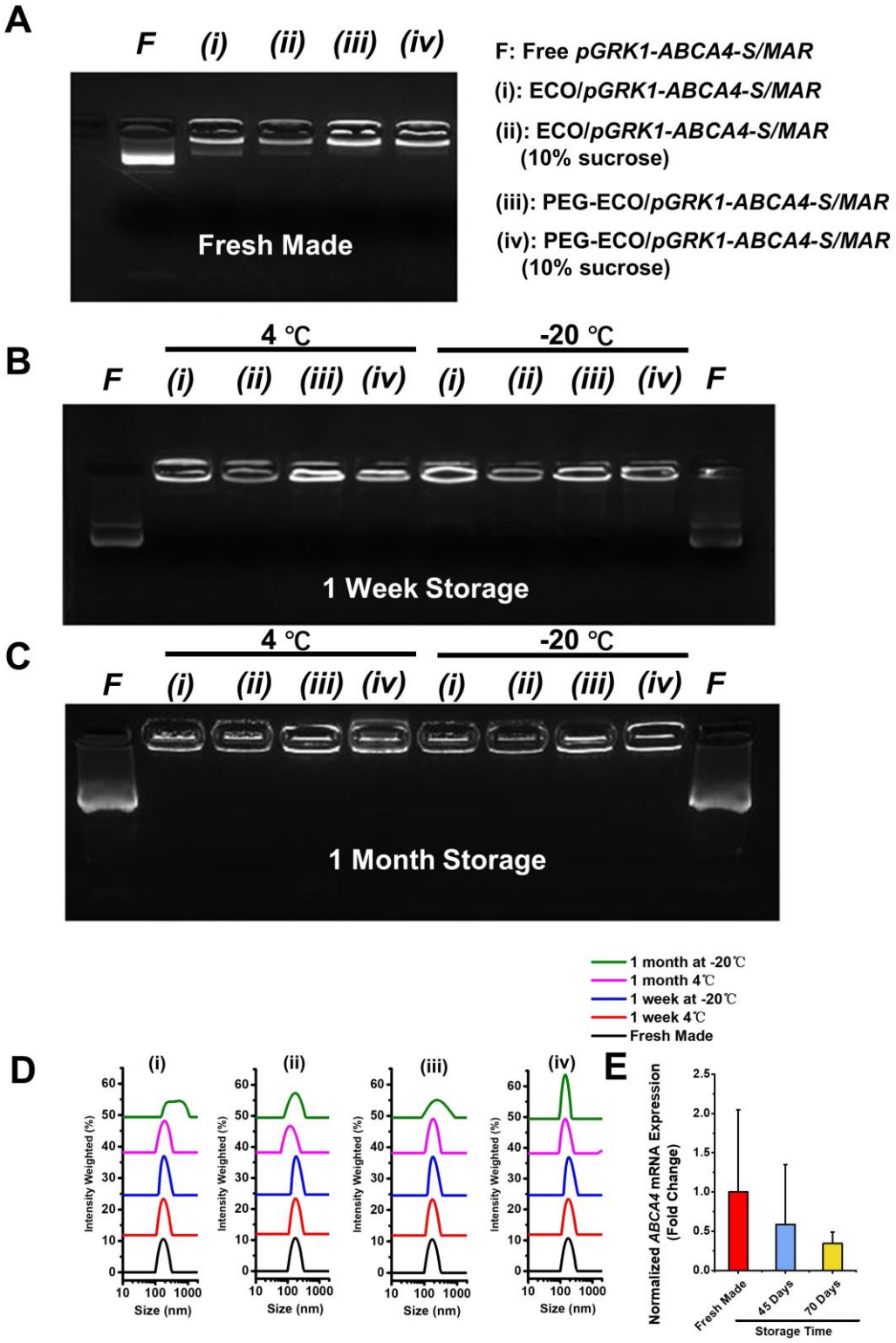

Fig. S2. Stability of ECO/*pGRK1-ABCA4-S/MAR* nanoparticle formulations. (A,B,C) Agarose gel electrophoresis and **(D)** nanoparticle size distribution of (i) ECO/*pGRK1-ABCA4-S/MAR,* (ii) ECO/*pGRK1-ABCA4-S/MAR* (10% sucrose), (iii) PEG-ECO/*pGRK1-ABCA4-S/MAR* and (iv) PEG-ECO/*pGRK1-ABCA4-S/MAR* (10% sucrose) nanoparticles under storage condition of 4 ℃ or -20 ℃ at day 0 (fresh made), day 7 and 1 month; **(E)** *ABCA4* mRNA

expression by qRT-PCR analysis of *Abca4*$^{-/-}$ mice treated with PEG-ECO/*pGRK1-ABCA4-S/MAR* (5% sucrose) nanoparticles (100 ng/eye) stored at -20℃ for 45 or 70 days. **(A)** is also shown in **Figure 1E**.

Table S1. Sizes and zeta potentials of ECO/*pGRK1-ABCA4-S/MAR* nanoparticle formulations

	Particle Size (nm)				
Formulations	**0 day**	**7 day 4℃**	**7 day -20℃**	**1 month day 4℃**	**1 month day -20℃**
ECO/*pGRK1-ABCA4-S/MAR*	186.46	199.43	200.5	198.8	427
PEG-ECO/*pGRK1-ABCA4-S/MAR*	189.74	189.12	210.5	200	211
ECO/*pGRK1-ABCA4-S/MAR* (10% Sucrose)	151.15	173.71	186.6	125.79	173.92
PEG-ECO/*pGRK1-ABCA4-S/MAR* (10% Sucrose)	174.06	182.53	174.67	175.28	171.11
	Zeta Potential (mV)				
Formulations	**0 day**	**7 day 4℃**	**7 day -20℃**	**1 month day 4℃**	**1 month day -20℃**
ECO/*pGRK1-ABCA4-S/MAR*	21.8	26.4	40.3	30.4	44.6
PEG-ECO/*pGRK1-ABCA4-S/MAR*	13.8	15.1	22.5	30.4	28.6
ECO/*pGRK1-ABCA4-S/MAR* (10% Sucrose)	21.9	25.5	49.8	39.8	45
PEG-ECO/*pGRK1-ABCA4-S/MAR* (10% Sucrose)	15.7	23	17.7	27.7	18.7

3. HPLC Analysis of A2E with sample chromatograms from mice received single treatment of different doses and multi-treatments.

A2E, composed of photo-toxic dimers of vitamin A, is a main component of lipofuscin [4, 5]. A2E accumulation is commonly used as an indicator of STGD progression [6]. One of the therapeutic strategies for treating STGD is to slow down the production and accumulation of A2E to minimize chronic oxidative damage that ultimately leads to atrophy. A2E accumulation gradually increased in *Abca4*$^{-/-}$ mice with aging, as has been demonstrated in our previous research [1]. A2E analysis was performed as described in the methods. The HPLC chromatograms were used to quantify relative A2E diminution compared with untreated controls. The area of the A2E peak was integrated and the peaks for treated mice were normalized to the peaks of control mice. The HPLC chromatograms are summarized for mice treated with a single dose (50 ng or 100 ng/eye) of PEG-ECO/*pGRK1-ABCA4-S/MAR* nanoparticles, **Fig. S3** (4 months after treatment), **Fig. S4 (**8 months after treatment), and **Fig. S5** (1 year after treatment).

For multiple treatments, the HPLC chromatograms are summarized in **Fig. S6** for mice treated with a single dose (100 ng/eye), 2 doses (2×100 ng/eye, at a3 months interval) or 3 doses (3×100 ng/eye, at 3 month intervals) of PEG-ECO/*pGRK1-ABCA4-S/MAR* nanoparticles. From the chromatograms, smaller A2E peaks could be observed in the treated groups *versus*

the control groups, especially for the multiple treatment groups. The quantitative analysis was presented in the manuscript **Fig. 2G** and **Fig. 3F**.

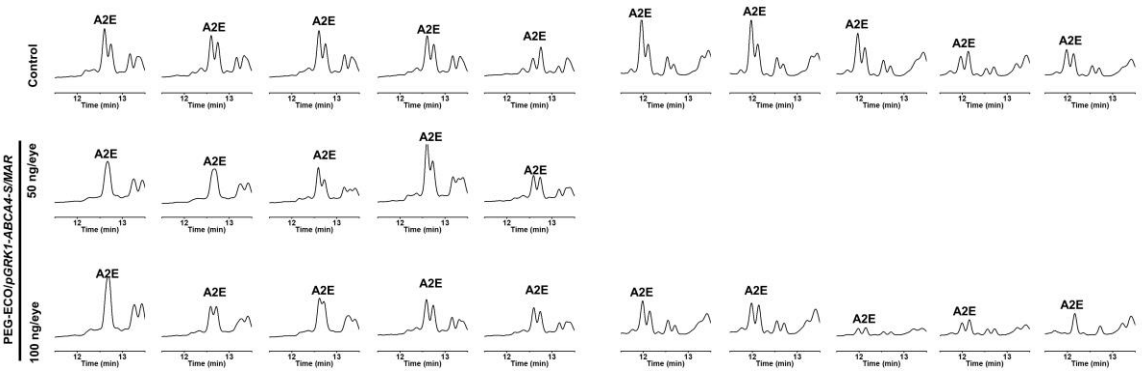

Fig. S3. Four months efficacy of PEG-ECO/ *pGRK1-ABCA4-S/MAR* nanoparticles for preventing A2E accumulation in *Abca4*$^{-/-}$ mice. HPLC chromatograms showing A2E peaks from control and nanoparticle-treated *Abca4*$^{-/-}$ mice 4 months after a single dose (50 ng or 100 ng/eye) of PEG-ECO/ *pGRK1-ABCA4-S/MAR* nanoparticles.

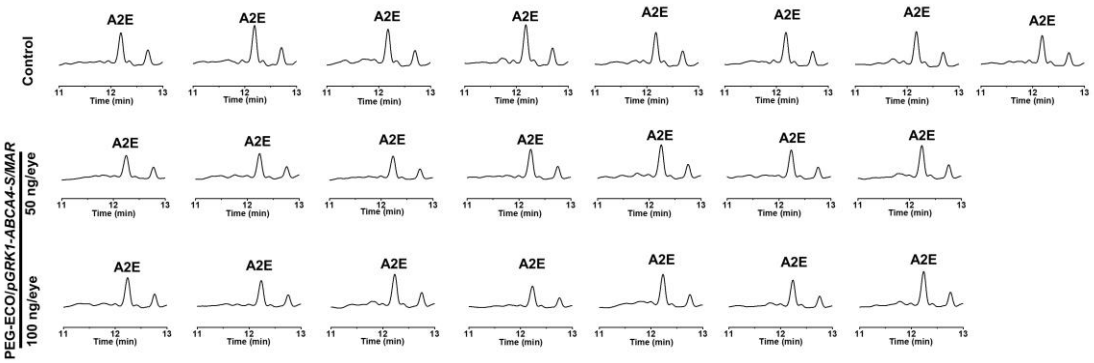

Fig. S4. Eight month efficacy of PEG-ECO/ *pGRK1-ABCA4-S/MAR* nanoparticles for preventing A2E accumulation in *Abca4*$^{-/-}$ mice. HPLC chromatograms showing A2E peaks from control and nanoparticle-treated *Abca4*$^{-/-}$ mice 8 months after a single dose (50 ng or 100 ng/eye) of PEG-ECO/ *pGRK1-ABCA4-S/MAR* nanoparticles.

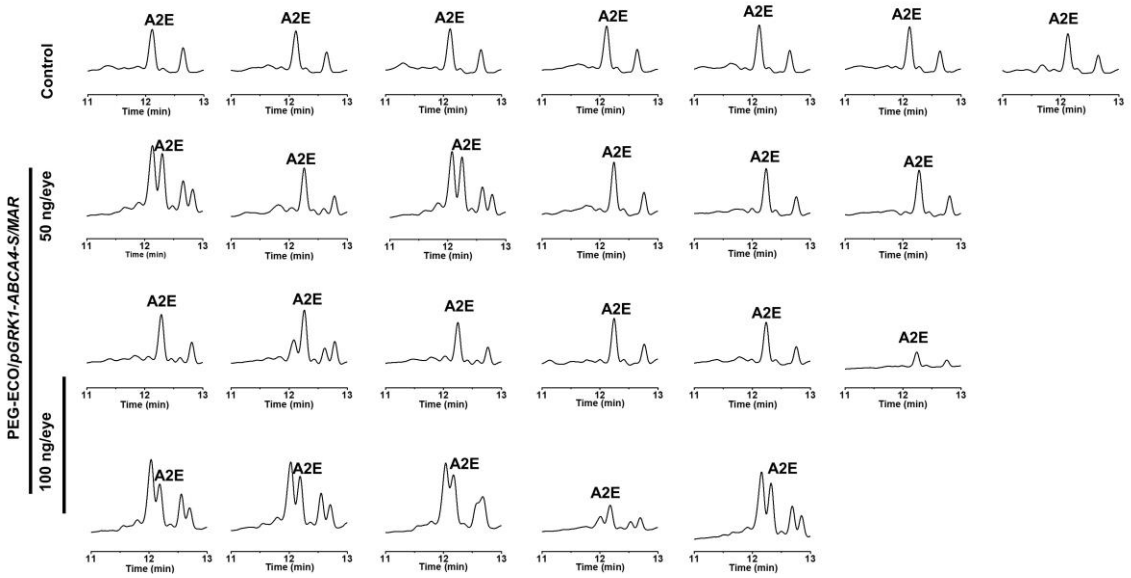

Fig. S5. One year efficacy of PEG-ECO/ *pGRK1-ABCA4-S/MAR* nanoparticles for preventing A2E accumulation in *Abca4*$^{-/-}$ mice. HPLC chromatograms showing A2E peaks from control and nanoparticle-treated *Abca4*$^{-/-}$ mice 1 year after a single dose (50 ng or 100 ng/eye) of PEG-ECO/ *pGRK1-ABCA4-S/MAR* nanoparticles.

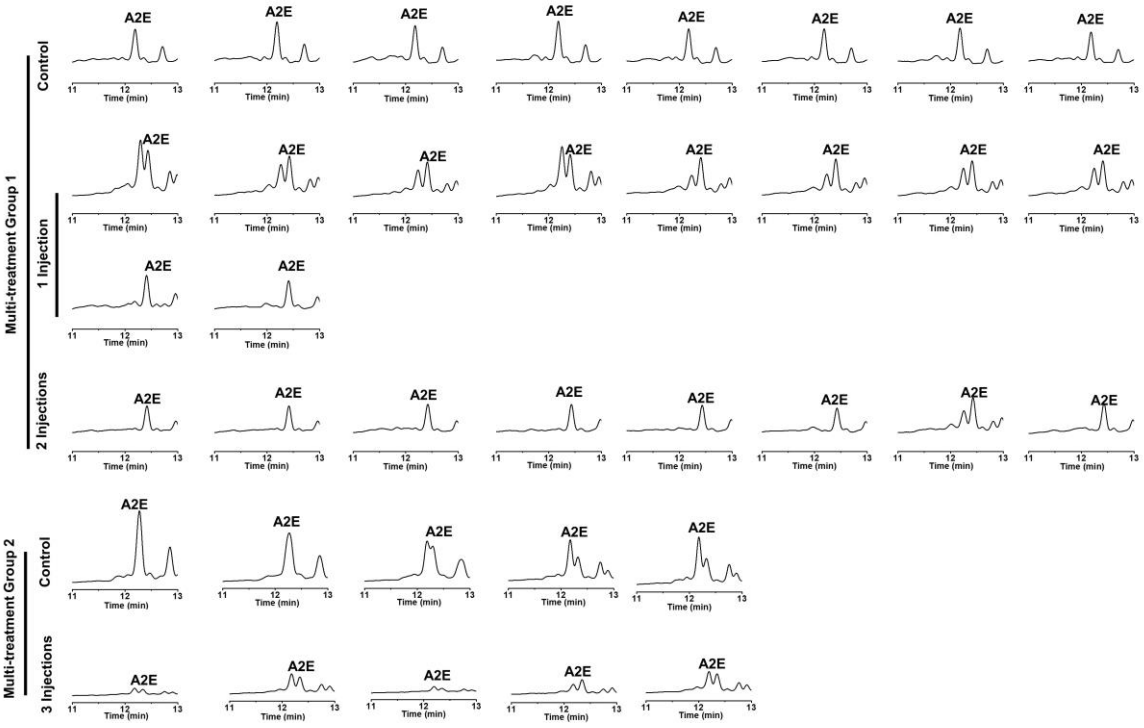

Fig. S6. Efficacy demonstrated by inhibition of A2E accumulation after multiple treatments with PEG-ECO/*pGRK1-ABCA4-S/MAR* nanoparticles (at 3 month intervals, 100 ng/eye). HPLC chromatograms showing A2E peaks from control and nanoparticle treated *Abca4*$^{-/-}$ mice.

Mice with 1 injection were sacrificed 8 months after injection; mice with 2 injections were sacrificed 5 months after the 2nd injection (8 months after the initial treatment); and mice with 3 injections were sacrificed 5 months after the 3rd injection.

The amount of A2E in the retinas of *Abca4*$^{-/-}$ mice after multi-treatments are summarized in **Fig. S7**. The quantification was based on HPLC analysis of A2E standard with a known concentration.

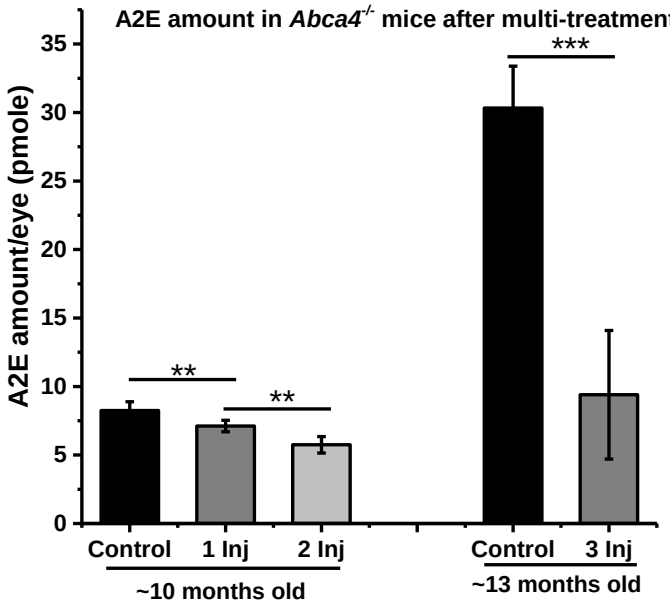

Figure S7. A2E amount (pmoles/eye) in the eyes of *Abca4*$^{-/-}$ mice after multi-treatments of gene therapy using PEG-ECO/*pGRK1-ABCA4-S/MAR* nanoparticles (every 3 months, 100 ng/eye). Mice with 1 injection were sacrificed 8 months after injection, mice with 2 injections were sacrificed 5 months after the 2nd injection (8 months after the initial treatment), the mice age was around 10 months when analyzed; Mice with 3 injections were sacrificed 5 months after the 3rd injection, the mice age was around 13 months when analyzed (** $p < 0.01$; ***$p<0.005$).

4. Safety of PEG-ECO/*pGRK1-ABCA4-S/MAR* nanoparticles

The cytotoxicity of ECO/*pGRK1-ABCA4-S/MAR* and PEG-ECO/*pGRK1-ABCA4-S/MAR* nanoparticles was first evaluated *in vitro* in ARPE-19 cells. Briefly, ECO/*pGRK1-ABCA4-S/MAR* nanoparticles were formulated at N/P ratios of 6 and 8 (see methods for detailed procedures). The nanoparticles were also tested after PEGylation using 2.5 mol% PEG, or

addition of 5% sucrose separately at an N/P ratio of 8. The cytotoxicity of ECO/*pGRK1-ABCA4-S/MAR* nanoparticles was evaluated at different *pDNA* doses (800 ng, 400 ng, 200 ng, 100 ng, 50 ng, 25 ng, 12.5 ng in 100 µL of transfection media) in ARPE-19 cells. ARPE-19 cells were seeded on a 96-well plate at 10,000 cells/well. Cells were treated with ECO/*pGRK1-ABCA4-S/MAR* and ECO/*pGRK1-ABCA4-S/MAR* (with 2.5 mol% PEG or 5% sucrose) nanoparticles for 4 hr, and the transfection medium was replaced with fresh medium. Cells were further incubated until 48 hr after transfection. The CCK-8 assay was used to evaluate cell viability after 48hr. The results are summarized in **Fig. S8.** ECO/*pGRK1-ABCA4-S/MAR* nanoparticles demonstrated dose-dependent cytotoxicity; for most doses of both N/P ratios, the nanoparticle formulations displayed low toxicity. Also, the N/P=6 formulation seemed to have lower cytotoxicity compared with N/P=8 (**Fig. S8A**). When PEGylation (2.5 mol% PEG) or 5% sucrose was incorporated into ECO/*pGRK1-ABCA4-S/MAR* nanoparticles, no obvious cytotoxicity was observed for the formulations across all the doses at N/P=8 **(Fig. S8B)**.

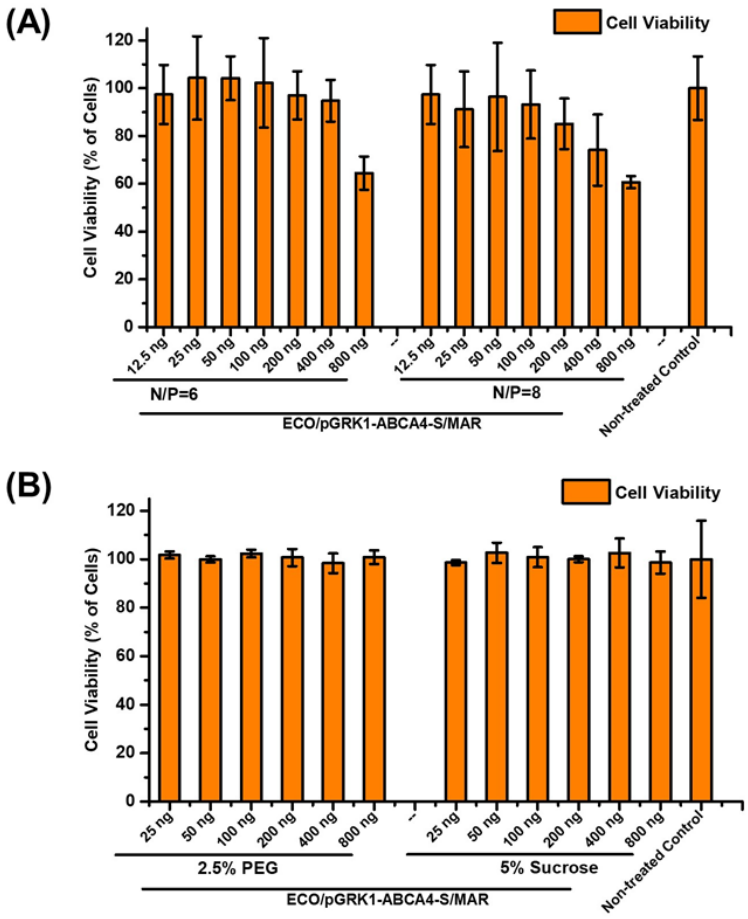

Fig. S8. *In vitro* cytotoxicity of the formulations of ECO/*pGRK1-ABCA4-S/MAR* nanoparticles. Cytotoxicity assessed by ARPE-19 cell viability 48 hr after transfection with ECO/*pGRK1-ABCA4-S/MAR* nanoparticles at N/P ratios of 6 and 8 **(A)** and with ECO/*pGRK1-ABCA4-S/MAR* nanoparticles formulated at N/P = 8 in 2.5% PEG or 5% sucrose **(B)**. Transfections were performed with *pDNA* doses of 800, 400, 200, 100, 50, 25, and 12.5 ng/100 µL media.

In vivo safety was evaluated using scotopic and photopic electroretinogram (ERG) responses after treatment with ECO/*pGRK1-ABCA4-S/MAR* in wild type *BALB/c* mice. A total of 5 *BALB/c* mice were injected with ECO/*pGRK1-ABCA4-S/MAR* nanoparticles formulated at a N/P=8 and a *pDNA* concentration of 200 ng/µL. The nanoparticles (0.5 µL) were injected into the subretinal space of the right eye, and 0.5 µL of PBS was injected to the left eye as the control. The mice were evaluated 1 month after injection by both scotopic and photopic electroretinogram (ERG). Results are summarized in **Fig. S9**.

After subretinal injection of ECO/*pGRK1-ABCA4-S/MAR* nanoparticles, *BALB/c* mice displayed similar ERG responses with similar intensities for both particles and PBS control, across all the tested light intensities; all mice also did not display any changes in the waveforms (**Fig. S9**). Therefore, ECO/*pGRK1-ABCA4-S/MAR* nanoparticles demonstrated good *in vivo* safety and mild to no adverse effects to eye function 1 month after a single injection in wild type *BALB/c* mice.

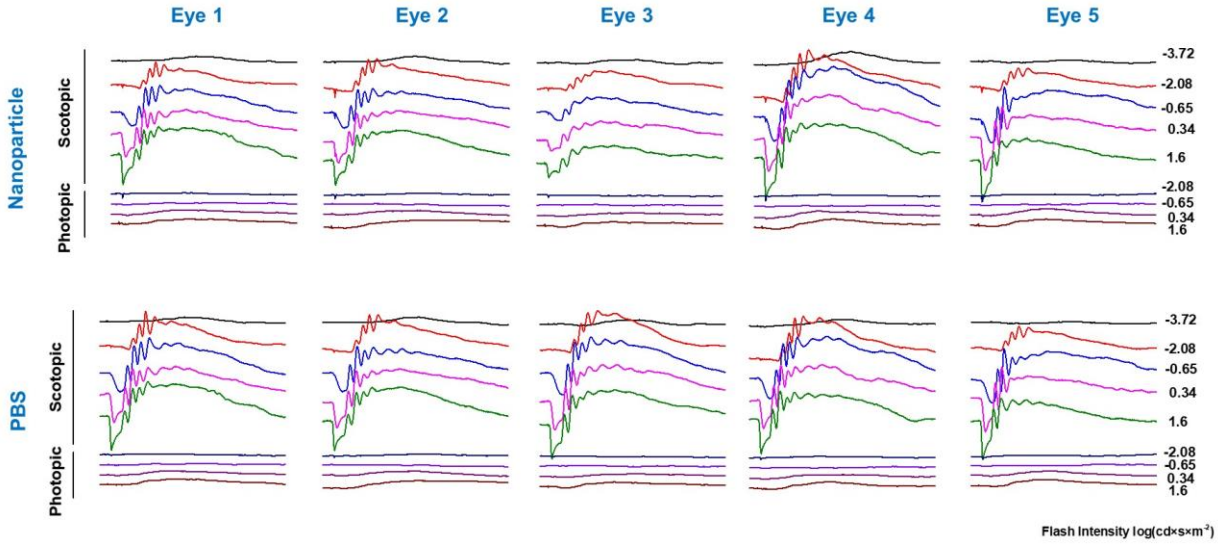

Fig. S9. Functional scotopic and photopic electroretinogram (ERG) analysis of *BALB/c* mice 1 month after subretinal injection of ECO/*pGRK1-ABCA4-S/MAR* nanoparticles at the test light intensities of -3.72~1.6 log(cd×s×m^{-2}).

Electroretinography (ERG) was also used to evaluate the eye function of *Abca4*$^{-/-}$ mice 10~10.5 months after the initial treatment, to assess the safety of treatment with PEG-ECO/*pGRK1-ABCA4-S/MAR* nanoparticles at a single dose (100 ng/eye) or 3 doses (3×100 ng/eye). Results are summarized in **Fig. S10**. No differences were observed in the ERG scotopic and photopic responses at the test intensity of 1.6 log(cd×s×m^{-2}) compared with the untreated control mice **(Fig. S10)**. Therefore, PEG-ECO/*pGRK1-ABCA4-S/MAR* nanoparticles demonstrated good *in vivo* safety both for single dose treatment and multiple treatments of *Abca4*$^{-/-}$ mice.

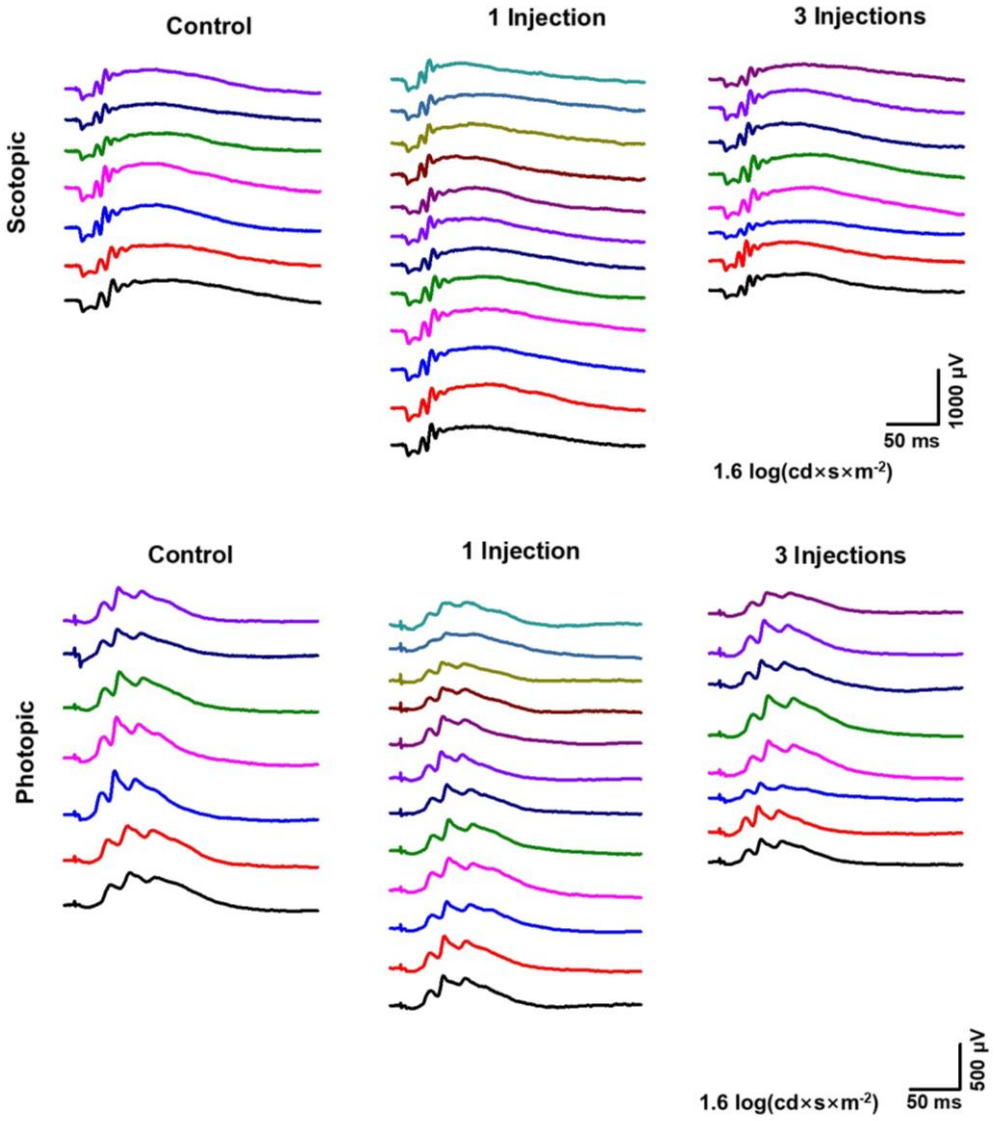

Fig. S10. Functional scotopic and photopic electroretinogram (ERG) analysis of *Abca4*$^{-/-}$ mice 10~10.5 months after the initial subretinal injection of 1 dose (100 ng/eye) or 3 doses (100 ng/eye at 3 month intervals) of PEG-ECO/*pGRK1-ABCA4-S/MAR* nanoparticles at the test light intensity of 1.6 log(cd×s×m^{-2}).

Using SLO in the fluorescent mode, we evaluated the morphology of the eyes of *Abca4*$^{-/-}$ mice 7 months after their initial treatment with multiple doses of ECO platform-based GRT using PEG-ECO/*pGRK1-ABCA4-S/MAR* nanoparticles. Results are summarized in **Fig. S11**. No treatment-associated adverse effects were observed for the 1-dose or 2-dose treatments compared with untreated control. Mice that received 3 doses seemed to have some injection-associated detachments (dark areas); however, these mice were tested only one month after the 3rd injection, so these detachments could have recovered if assessed at a later time.

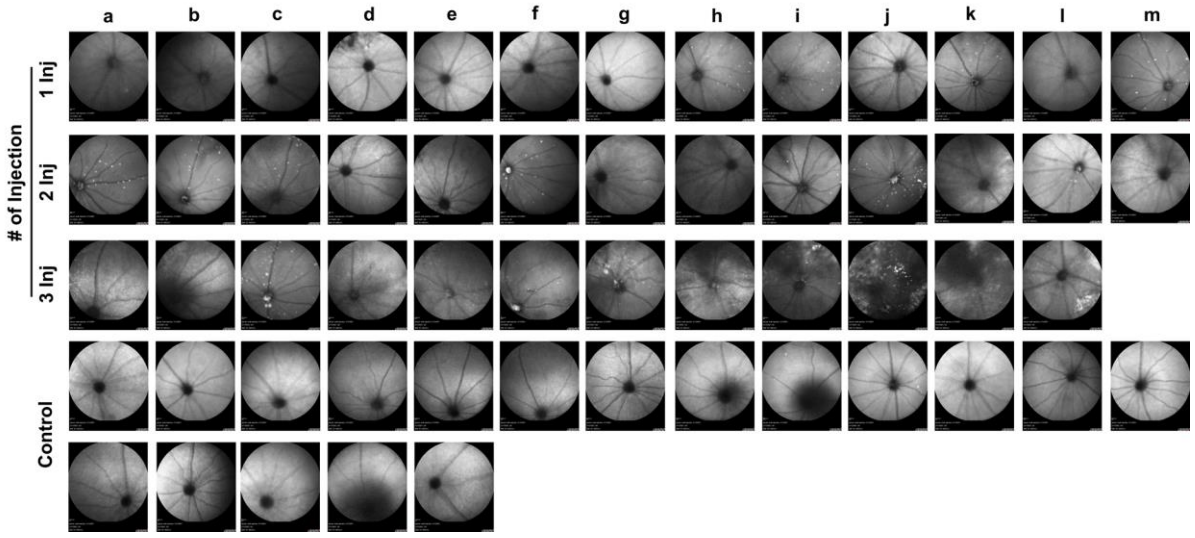

Fig. S11. Safety of PEG-ECO/*pGRK1-ABCA4-S/MAR* nanoparticles. Eye morphology was assessed 7 months after the first subretinal treatment (control: untreated) by fluorescent-scanning laser ophthalmoscopy (SLO), and fluorescent images are shown for *Abca4*$^{-/-}$ mice that received multiple doses of PEG-ECO/*pGRK1-ABCA4-S/MAR* nanoparticles. Mice were treated at 3 month intervals. SLO was performed 7 months after the initial injection (4 months after the 2nd injection, and 1 month after the 3rd injection). Selected SLO images are also shown in **Figure 4C**.

In vivo safety of the ECO/*pDNA* nanoparticles was also evaluated by morphology of the eye in comparison with AAV2. Briefly, ACU-PEG-HZ-ECO/*pCMV-GFP* nanoparticles (the ACU ligand was used to enhance interphotoreceptor matrix delivery) were formulated at N/P = 8 at a *pDNA* concentration of 46 ng/uL with 5% sucrose. The nanoparticles (0.5 uL) were injected into the subretinal space of one eye of a *BALB/c* mouse. The contralateral eye was injected with AAV2-CMV-GFP at an equivalent dose (calculated based on GFP copy number). Untreated mice were used as controls. Scanning laser ophthalmoscope (SLO, fluorescent mode) was used to evaluate the eye condition at 1, 2 and 3 months post injection using the fluorescent mode. Results are summarized in **Fig. S12**. AAV2 seemed to induce more lesions and potential inflammations than ECO nanoparticles, as demonstrated by the saturated white color regions. These results demonstrated the ECO/*pDNA* nanoparticles to have a potentially better safety profile.

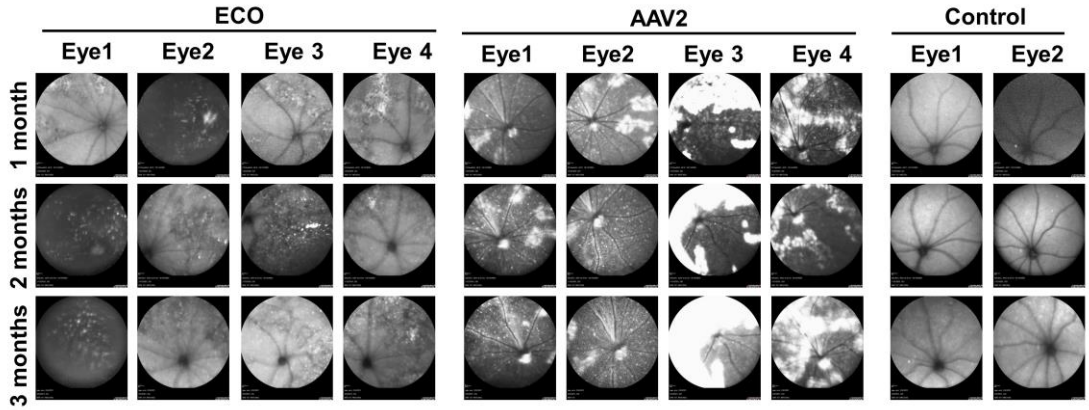

Fig. S12. Safety of EM-PEG-HZ-ECO/*pCMV-GFP* nanoparticles compared with AAV2 viral particles. Eye morphology of *BALB/c* mice treated with EM-PEG-HZ-ECO/*pCMV-GFP* nanoparticles or AAV2-CMV-GFP *versus* control (untreated) was assessed by fluorescent scanning laser ophthalmoscope (SLO) images of the eye 1, 2 and 3 months after treatments (all treated mice received the same dose by gene copy number). Selected SLO images are also shown in **Figure 4D**.

Table S2. Primer information

Name	Sequence 5'-3'
ABCA4 qPCR Forward	TCCAAGCACCTCCAGTTTATC
ABCA4 qPCR Reverse	CCCAGCACTCACGGAATAAT
18s internal control Forward	AGGATCCATTGGAGGGCAAGT
18s internal control Reverse	TCCAACTACGAGCTTTTTAACTGCA
ABCA4 genotyping Forward	TCTCGGGGATGTTTTGAGAC
ABCA4 genotyping Reverse	AATGGATCCACACCACCAAC
NEO-F	CGTTGGCTACCCGTGATATT
pGRK1 Forward	GGGCCCCAGAAGCCTGGTGGTTGTTTGTCCTTCTCAGG
pGRK1 Reverse	GCCCTTGCCTGTGGCCCGTCCCTGCCCTTGCTGG
MluI insertion Forward	CCGAAAAGTGCCACCTGACGCGTCGACATTGATTATTGAC
MluI insertion Reverse	GTCAATAATCAATGTCGACGCGTCAGGTGGCACTTTTCGG
NheI insertion Forward	AAGGCCGCGTTGCTAGCGTTTTTCCATAGGC
NheI insertion Reverse	GCCTATGGAAAAACGCTAGCAACGCGGCCTT
Globin polyA Forward	ACATTTGCTTCTGACACAACTGTGTTCACTAGCAACCTC
Globin polyA Reverse	GCAATGAAAATAAATGTTTTTTATTAGGCAGAATCCAGATGCTCAAGG
S/MAR Forward	TGCAACACCCCAGTAAAGAG
S/MAR Reverse	TAGCTAGCTCTATCAAGATATTTAAAGAAAAAAAAAATTGTATCAACTTTATACAATCTC

Reference

1. Sun, D, Schur, RM, Sears, AE, Gao, S-Q, Vaidya, A, Sun, W*, et al.* (2020). Non-viral Gene Therapy for Stargardt Disease with ECO/pRHO-ABCA4 Self-Assembled Nanoparticles. *Molecular Therapy* **28**: 293-303.
2. Sun, D, Sun, W, Gao, S-Q, Wei, C, Naderi, A, Schilb, AL*, et al.* (2021). Formulation and efficacy of ECO/pRHO-ABCA4-SV40 nanoparticles for nonviral gene therapy of Stargardt disease in a mouse model. *Journal of Controlled Release* **330**: 329-340.
3. Young, JE, Vogt, T, Gross, KW, and Khani, SC (2003). A Short, Highly Active Photoreceptor-Specific Enhancer/Promoter Region Upstream of the Human Rhodopsin Kinase Gene. *Investigative Ophthalmology & Visual Science* **44**: 4076-4085.
4. Radu, RA, Mata, NL, Bagla, A, and Travis, GH (2004). Light exposure stimulates formation of A2E oxiranes in a mouse model of Stargardt's macular degeneration. *Proceedings of the National Academy of Sciences of the United States of America* **101**: 5928-5933.
5. Kennedy, CJ, Rakoczy, PE, and Constable, IJ (1995). Lipofuscin of the retinal pigment epithelium: A review. *Eye* **9**: 763.
6. Radu, RA, Mata, NL, Nusinowitz, S, Liu, X, Sieving, PA, and Travis, GH (2003). Treatment with isotretinoin inhibits lipofuscin accumulation in a mouse model of recessive Stargardt's macular degeneration. *Proceedings of the National Academy of Sciences* **100**: 4742-4747.